Journal of Sound and Vibration (2002) **249**(1), 101–127
doi:10.1006/jsvi.2001.3830, available online at http://www.idealibrary.com on IDEAL®

FREE VIBRATIONS OF SELF-STRAINED ASSEMBLIES OF BEAMS

D. J. MEAD

Institute of Sound and Vibration Research, University of Southampton, Southampton SO17 1BJ, England. E-mail: djm@isvr.soton.ac.uk

(*Received* 5 *March* 2001, *and in final form* 13 *June* 2001)

This paper examines the natural frequencies and modes of transverse vibration of two simple redundant systems comprising straight uniform Euler–Bernoulli beams in which there are internal self-balancing axial loads (e.g., loads due to non-uniform thermal strains). The simplest system consists of two parallel beams joined at their ends and the other is a 6-beam rectangular plane frame. Symmetric mode vibration normal to the plane of the frame is studied. Transcendental frequency equations are established for the different systems. Computed frequencies and modes are presented which show the effect of (1) varying the axial loads over a wide range, up to and beyond the values which cause individual members to buckle (2) pinning or fixing the beam joints (3) varying the relative flexural stiffness of the component beams. When the internal axial loads first cause any one of the component beams to buckle, the fundamental frequency of the whole system vanishes. The critical axial loads required for this are determined. A simple criterion has been identified to predict whether a small increase from zero in the axial compressive load in any one member causes the natural frequencies of the whole system to rise or fall. It is shown that this depends on the relative flexural stiffnesses and buckling loads of the different members. Computed modes of vibration show that when the axial modes reach their critical values, the buckled beam(s) distort with large amplitudes while the unbuckled beam(s) move either as rigid bodies or with bending which decays rapidly from the ends to a near-rigid-body movement over the central part of the beam. The modes of the systems with fixed joints change very little (if at all) with changing axial load, except when the load is close to the value which maximizes or minimizes the frequency. In a narrow range around this load the mode changes rapidly. The results provide an explanation for some computed results (as yet unpublished) for the flexural modes and frequencies of flat plates with non-uniform thermal stress distributions.

1. INTRODUCTION

It is well known that natural frequencies of flexural vibration increase when beams are stretched by axial tensile loads and they decrease when the axial loads are compressive. When the compression approaches the critical load for static instability of the beam, the fundamental frequency of the beam tends to zero. Vibrations of stretched beams were analyzed as long ago as the mid-19th century [1], the relevance of the work then being seen primarily in relation to stringed musical instruments—how did the flexural stiffness of a stretched string affect its tone?

The importance of axial compression on beam vibration has been recognized in the context of building vibration, especially in relation to earthquake-excited vibration. The lateral vibration modes of tall buildings have natural frequencies which are affected by

0022-460X/02/010101 + 27 $35.00/0

compressive loads in the vertical columns. Accordingly, many papers have considered the vibrations of compressed beam-columns and a few of them are cited [2–9]. The more recent of these have focussed on the effects on the modes and frequencies of the column boundary condition, its degree of taper, shear flexibility, etc. Some have sought simple formulae to predict the frequencies.

The vibration of a more complicated structure under compression was studied by Howson and Williams [10]. It took the form of an H-frame with fixed joints, compressed equally along the vertical side members which were considered as Timoshenko columns. Natural frequencies calculated for the whole system at different compression loads compared well with experimental results. Most structures, however, have some members which are compressed and some which are stretched, the compression and tension loads being linearly related. A simple plane frame or truss under static load is one example of these. When the wavelengths of their "overall" vibration modes are much greater than the lengths of the individual members, the corresponding natural frequencies are little affected by the static axial loads in its members provided the members remain straight. However, the frequencies of short wavelength modes (i.e., half-wavelengths comparable with or less than member lengths) which are normally very high may be much more affected. Indeed, one of them will drop to zero when the compression load in a member approaches the critical load of the member. Conversely, the frequencies of such modes will increase if the tension loads in all the structural members can be increased. This invites the question of the effect on frequencies and modes when some members are compressed at the same time as others are stretched. Do the frequencies rise or fall?

A partial answer to this has been sought in this paper through a study of two very simple redundant beam and frame-type structures. Being redundant, they can be "internally self-loaded", i.e., steady self-balancing axial loads can exist in the members in the absence of any external loads on the structure. Some of the members will be in tension and some in compression, a real situation which can be created by non-uniform thermal strains within the structure or by an initial lack of fit of any redundant member. Steady internal moments may also exist in such a structure (as in a portal frame) but only steady axial loads will be dealt with in this paper.

The particular structures considered are simple assemblies of straight and uniform beams, the vibrations of which are all governed by the simple linear Euler–Bernoulli beam equation. The effects of shear deflection, rotatory inertia and large deflection are therefore all ignored. A brief review is first presented on the theory of single beams with axial loading and with various boundary conditions. Curves of their frequencies are presented. A single pair of parallel beams, joined at their ends and with mutually interacting tensile and compressive axial loads is next considered. This impractical example could be made of one tubular beam, enclosing and joined at its ends to another beam which is free to vibrate (almost) independently. A six-beam rectangular frame with four outer beams and two internal diagonal beams is finally considered. The joints at the four corners are considered firstly to be pinned and then to be fully fixed. Vibration normal to the plane of the frame is studied. It has been found for both structures that as the internal self-balancing loads increase from zero, the frequencies may initially rise or fall before they eventually drop to zero.

The redundant six-beam frame has been chosen as a qualitative illustrator of a free–free rectangular plate which is hotter at its centre than at its edges. In-plane thermal stresses exist in such a plate which are compressive over the plate centre but are tensile around its edges. These stresses change the frequencies of transverse flexural motion, one of which vanishes as a critical temperature is approached. The six-beam frame which is hotter in the centre than at the edges has compressive stresses in the diagonals and tension stresses in the

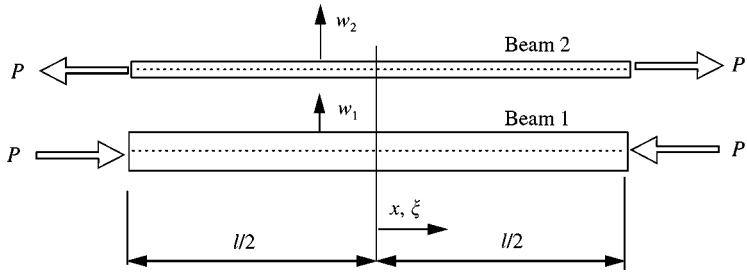

Figure 1. Displacement and co-ordinate systems used for the pair of axially loaded beams.

edge members and one of its natural frequencies is shown to vanish as the axial load in a diagonal approaches a critical buckling load. The general effect of internal stress on the transverse vibrations of the plate are therefore similar in nature to the effect of internal member loads on the transverse vibrations of the frame. The author undertook the current simpler study of beam-frame assemblies in order to explain phenomena of the plate problem observed in his studies. The latter will be reported in a later paper.

2. SINGLE AXIALLY LOADED UNIFORM BEAMS; EQUATIONS OF MOTION, MODES AND FREQUENCIES

2.1. GENERAL EQUATIONS

As the more complicated system of a self-strained frame has some members in compression and others in tension, it is appropriate initially to develop parallel theories for a single beam in compression and one of different mass and stiffness in tension. The theory for one, of course, is easily derived from the other by simply changing the sign of the axial load and the suffices of the mass and stiffness parameters. The theories are by no means new (see references [1–11]) but a separate parallel development with different notation for each beam is helpful at this stage as an introduction to later sections of this paper.

Figure 1 shows the two beams and the displacement and co-ordinate systems to be used. Beam 1 has the positive axial compressive load of P and beam 2 has the positive axial tensile load of P. EI_1 and EI_2 are the flexural rigidities and m_1 and m_2 are the masses per unit length of the two beams. (A list of symbols is given in Appendix B.)

The equations of free motion of the beams have the well-known forms

$$EI_1 \frac{\partial^4 w_1}{\partial x^4} = -m_1 \frac{\partial^2 w_1}{\partial t^2} - P \frac{\partial^2 w_1}{\partial x^2}, \quad EI_2 \frac{\partial^4 w_2}{\partial x^4} = -m_2 \frac{\partial^2 w_2}{\partial t^2} + P \frac{\partial^2 w_2}{\partial x^2} \qquad (1a,b)$$

which, with simple harmonic motion at frequency ω, become

$$EI_1 \frac{d^4 w_1}{dx^4} + P \frac{d^2 w_1}{dx^2} - \omega^2 m_1 w_1 = 0 \quad \text{and} \quad EI_2 \frac{d^4 w_2}{dx^4} - P \frac{d^2 w_2}{dx^2} - \omega^2 m_2 w_2 = 0. \qquad (2a,b)$$

These will be expressed in non-dimensional form by dividing the first by EI_1, the second by EI_2, and by making use of the following non-dimensional parameters:

$$\xi = \frac{x}{l}, \quad p = \frac{Pl^2}{EI_1}, \quad \Omega^2 = \frac{m_1 l^4}{EI_1}\omega^2, \quad e_{21} = \frac{EI_2}{EI_1}, \quad \mu_{21} = \frac{m_2}{m_1}. \tag{3a–d}$$

The equations then become

$$\frac{\mathrm{d}^4 w_1}{\mathrm{d}\xi^4} + p\frac{\mathrm{d}^2 w_1}{\mathrm{d}\xi^2} - \Omega^2 w_1 = 0, \quad \frac{\mathrm{d}^4 w_2}{\mathrm{d}\xi^4} - p\frac{1}{e_{21}}\frac{\mathrm{d}^2 w_2}{\mathrm{d}\xi^2} - \frac{\mu_{21}}{e_{21}}\Omega^2 w_2 = 0 \tag{4a,b}$$

which admit the solutions $w_1 = A\exp\alpha\xi$ and $w_2 = B\exp\beta\xi$. The numbers α and β are the roots of the bi-quadratic equations

$$\alpha^4 + p\alpha^2 - \Omega^2 = 0 \quad \text{and} \quad \beta^4 - p\frac{1}{e_{21}}\beta^2 - \frac{\mu_{21}}{e_{21}}\Omega^2 = 0 \tag{5a,b}$$

of which the solutions are

$$\alpha_1 = \pm\sqrt{-\frac{p}{2} + \sqrt{\left(\frac{p}{2}\right)^2 + \Omega^2}}, \quad \alpha_2 = \pm\sqrt{-\frac{p}{2} - \sqrt{\left(\frac{p}{2}\right)^2 + \Omega^2}}, \tag{6a,b}$$

$$\beta_1 = \pm\sqrt{\frac{p}{2}\frac{1}{e_{21}} + \sqrt{\left(\frac{p}{2}\frac{1}{e_{21}}\right)^2 + \frac{\mu_{21}}{e_{21}}\Omega^2}}, \quad \beta_2 = \pm\sqrt{\frac{p}{2}\frac{1}{e_{21}} - \sqrt{\left(\frac{p}{2}\frac{1}{e_{21}}\right)^2 + \frac{\mu_{21}}{e_{21}}\Omega^2}}. \tag{7a,b}$$

Notice that when the beams are identical ($e_{21} = 1$)

$$\alpha_1^2 = -\beta_2^2, \quad \alpha_2^2 = -\beta_1^2, \tag{8a,b}$$

but for all values of e_{21}

$$\alpha_2^2 + \alpha_1^2 = -p, \quad \beta_2^2 + \beta_1^2 = +\frac{p}{e_{21}}. \tag{8c,d}$$

The analysis and results of this paper will be restricted to beams and natural modes which are symmetric about the beam centres, i.e., the beams have the same boundary conditions at each end and the modes of vibration are expressible in terms of the even hyperbolic functions

$$w_1 = A_1\cos\alpha_1\xi + A_2\cos\alpha_2\xi \quad \text{and} \quad w_2 = B_1\cosh\beta_1\xi + B_2\cosh\beta_2\xi. \tag{9a,b}$$

The natural frequencies of the vibrating beams and the modes (the ratios of the A's and B's) are found in the usual way from equations expressing the four boundary conditions of the beams. On account of the symmetry restriction, satisfaction of these conditions at $\xi = +1/2$ automatically ensures their satisfaction at $\xi = -1/2$. This feature, of course, reduces the computational effort required in finding modes and frequencies.

2.2. BEAMS WITH PARTICULAR BOUNDARY CONDITIONS

It is well known that beams with simply supported ends vibrate in simple cosinusoidal modes which satisfy the necessary boundary conditions of zero displacement and zero

curvature at each end. Hence, by writing $w_1(x)$, $w_2(x) = C_n \cos(2n-1)\,\pi x/l$, $(n \geqslant 1)$ and substituting these directly into equations (4a,b) leads to the frequency equation for the compressed beam

$$\Omega_{1,n} = (2n-1)\,\pi\sqrt{(2n-1)^2\pi^2 - p} \tag{10a}$$

in which p is +ve for a compressive load.

For the stretched beam

$$\Omega_{2,n} = (2n-1)\,\pi\sqrt{\frac{e_{21}}{\mu_{21}}}\sqrt{(2n-1)^2\pi^2 + \frac{p}{e_{21}}} \tag{10b}$$

in which p is +ve for a tensile load.

The frequency of the compressed beam clearly vanishes when $\sqrt{p} = (2n-1)\pi$, i.e., when $P_n = +(\pi^2 EI_1/l^2)(2n-1)^2$ $(n = 1$ to $\infty)$. These P_n values are the critical buckling loads of the strut, of which the lowest $(P_1 = \pi^2 EI_1/l^2)$ alone has any practical significance. The fundamental frequency of the stretched beam vanishes when its axial load is negative with the value $-\pi(EI_1/l^2)\,e_{21}$.

When the ends of the beams are fully fixed, the modes of vibration are given by equations (9a) or (9b) subject to the boundary conditions $w = 0$ and $\mathrm{d}w/\mathrm{d}x = 0$ at $\xi = \pm 1/2$. When $e_{21} = 1 = \mu_{21}$, the frequency equations for the compressed and stretched beams are then found to be

$$\alpha_1 \tanh \alpha_1/2 - \alpha_2 \tanh \alpha_2/2 = 0 \quad (p \text{ +ve for a compressive load}), \tag{11a}$$

$$\beta_1 \tanh \beta_1/2 - \beta_2 \tanh \beta_2/2 = 0 \quad (p \text{ +ve for a tensile load}). \tag{11b}$$

For a beam with no axial load $(p = 0)$, $\alpha_1 = \mathrm{i}\alpha_2$, $\beta_1 = \mathrm{i}\beta_2$ and these equations lead to well-known forms involving $\tan \alpha_1/2$ and $\tan \beta_1/2$. This is no longer true when the beams are compressed or stretched. Equations (11a,b) are then best left as above.

When both ends of the beams are free, the bending moments are at the ends are zero so $\mathrm{d}^2w/\mathrm{d}x^2 = 0$ at $\xi = \pm 1/2$. The total transverse force acting on each end of the beam must also be zero. This consists of more than the shear force $EI\,(\mathrm{d}^3w/\mathrm{d}x^3)$, as the direction of the axial load within the beam is along the line of the deflected neutral surface. A compression load of P at the right-hand end is therefore inclined to the horizontal by $\mathrm{d}w/\mathrm{d}x$ and has the downwards transverse component $P(\mathrm{d}w/\mathrm{d}x)$. Hence, the total downwards force on the right-hand end is $EI\,(\mathrm{d}^3w/\mathrm{d}x^3) + P(\mathrm{d}w/\mathrm{d}x)$ and the boundary conditions to be satisfied for beams 1 and 2 are

$$\frac{\mathrm{d}^2 w_{1,2}}{\mathrm{d}x^2} = 0, \quad \frac{\mathrm{d}^3 w_1}{\mathrm{d}\xi^3} + p\frac{\mathrm{d}w_1}{\mathrm{d}\xi} = 0, \quad \frac{\mathrm{d}^3 w_2}{\mathrm{d}\xi^3} - \frac{p}{e_{21}}\frac{\mathrm{d}w_2}{\mathrm{d}\xi} = 0, \quad \text{all at } \xi = \pm\,1/2. \tag{12a–c}$$

Substitution of the displacement expressions (9a) or (9b) into these boundary conditions leads to the following frequency equations for free–free beams:

$$\alpha_1^3 \tanh \alpha_2/2 - \alpha_2^3 \tanh \alpha_1/2 = 0 \quad (p \text{ +ve for a compressive load}) \tag{13a}$$

and

$$\beta_1^3 \tanh \beta_2/2 - \beta_2^3 \tanh \beta_1/2 = 0 \quad (p \text{ +ve for a tensile load}). \tag{13b}$$

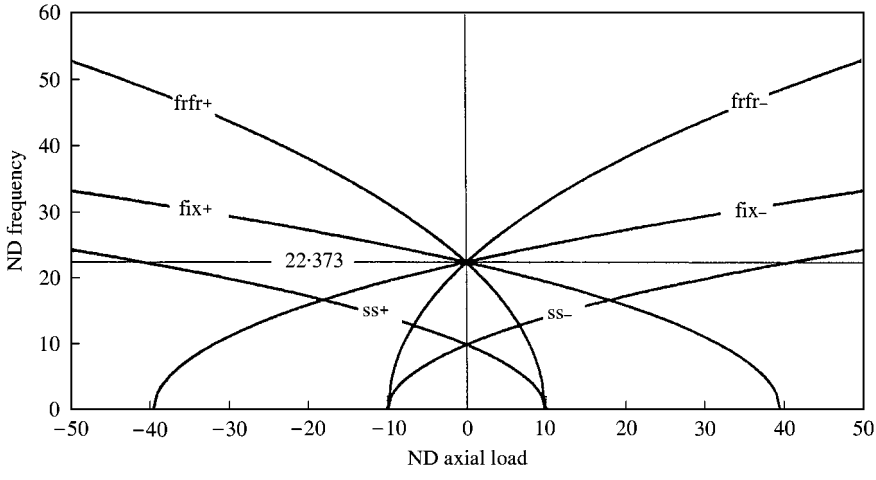

Figure 2. Natural frequencies versus ND axial load for single axially loaded uniform beams with various boundary conditions. $e_{21} = 1$. frfr = free–free beam; fix = fully fixed beam; ss = simply supported beam: + signifies that a positive axial load is compressive; − signifies a negative axial load is compressive.

Calculated values of the frequencies for these six beams with $e_{21} = 1$ are shown in Figure 2, the curves of which correspond in form and value with some of Bokaian's curves [8, 11]. Each curve for a compressed beam is the exact image (mirrored in the frequency axis) of the curve for the stretched beam. The values of p at which the frequencies vanish for each beam are clearly apparent. The frequencies of the simply supported and the free–free beams both vanish at the same ND axial load values of $\pm\pi^2$ which correspond to the critical buckling loads for both beams. It makes no difference to this whether the ends of the beam are pinned or free. On the other hand, when the ends of the beam are fixed, the frequency vanishes when $p = \pm 4\pi^2$ which corresponds to the well-known critical buckling load of a fully fixed beam.

3. PAIRS OF PARALLEL BEAMS JOINED TOGETHER

3.1. BEAMS PINNED AT THEIR ENDS

A schematic diagram of the pair of beams and the co-ordinate system to be used is shown in Figure 3(a). The distance between the assembled end joints is l and the (different) flexural displacements of the two beams are w_1 and w_2. Figure 3(b) shows the interacting axial forces and moments at the right-hand ends of the beam which may be caused either by differential thermal strains or by the beams being initially of unequal length.

The following boundary conditions apply in this case:

(1) equal displacements of the beams at each end:

$$w_1 = w_2 \quad \text{at } \xi = \pm 1/2; \tag{14a}$$

(2) zero bending moment (i.e., zero curvature) in each beam at each end:

$$d^2w_1/d\xi^2 = 0 \quad \text{at } \xi = \pm 1/2 \quad \text{and} \quad d^2w_2/d\xi^2 = 0 \quad \text{at } \xi = \pm 1/2; \tag{14b,c}$$

(3) zero total transverse force on the beams at each end.

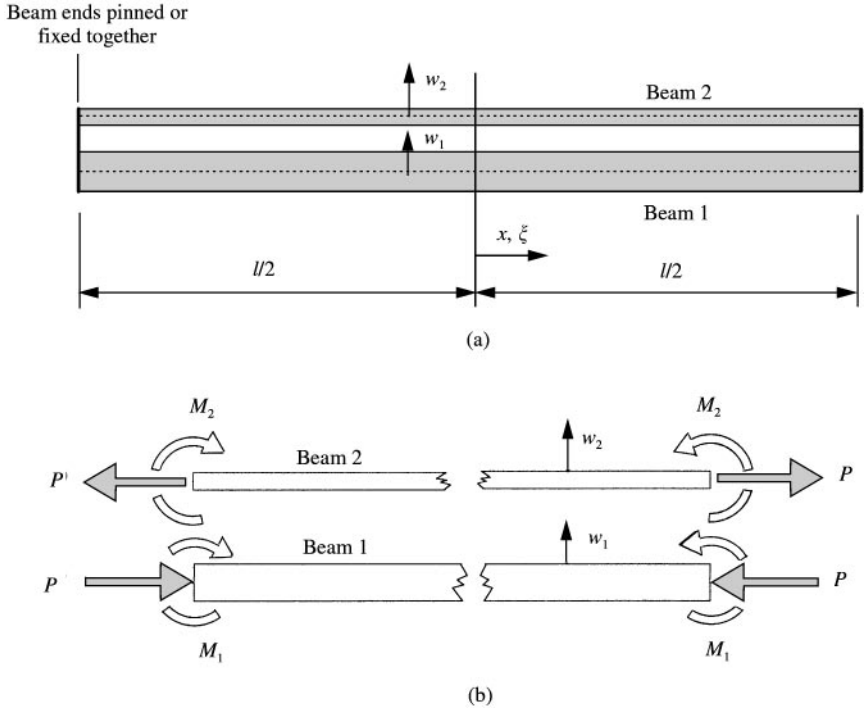

Figure 3. (a) Schematic diagram of the pair of joined beams and the co-ordinate system used; (b) the interacting axial forces at the ends of the beams.

As for the single free–free beam, there is more to this than the vanishing of the total shear force $\sum_{n=1}^{2} EI_n \, \mathrm{d}^3 w_n/\mathrm{d}x^3$ in the beams. The vertical component of the axial loads in the beams must be added into it and this yields the equation

$$EI_1 \frac{\mathrm{d}^3 w_1}{\mathrm{d}x^3} + P\frac{\mathrm{d}w_1}{\mathrm{d}x} + EI_2 \frac{\mathrm{d}^3 w_2}{\mathrm{d}x^3} - P\frac{\mathrm{d}w_2}{\mathrm{d}x} = 0 \quad \text{at } x = \pm 1/2,$$

which has the non-dimensional form

$$\frac{\mathrm{d}^3 w_1}{\mathrm{d}\xi^3} + p\frac{\mathrm{d}w_1}{\mathrm{d}\xi} + e_{21}\frac{\mathrm{d}^2 w_2}{\mathrm{d}\xi^3} - p\frac{\mathrm{d}w_2}{\mathrm{d}\xi} = 0 \quad \text{at } \xi = \pm 1/2. \tag{14d}$$

Substitution of equations (9a, b) into equations (14a–d) yields the matrix equation

$$\begin{bmatrix} \cosh\alpha_1/2 & \cosh\alpha_2/2 & -\cosh\beta_1/2 & -\cosh\beta_2/2 \\ \alpha_1^2\cosh\alpha_1/2 & \alpha_2^2\cosh\alpha_2/2 & 0 & 0 \\ 0 & 0 & \beta_1^2\cosh\beta_1/2 & \beta_2^2\cosh\beta_2/2 \\ a_{1p}\sinh\alpha_1/2 & a_{2p}\sinh\alpha_2/2 & b_{1p}\sinh\beta_1/2 & b_{2p}\sinh\beta_2/2 \end{bmatrix} \begin{Bmatrix} A_1 \\ A_2 \\ B_1 \\ B_2 \end{Bmatrix} = 0, \tag{15}$$

where

$$a_{1p} = (\alpha_1^3 + \alpha_1 p) = -\alpha_1\alpha_2^2, \quad a_{2p} = (\alpha_2^3 + \alpha_2 p) = -\alpha_1^2\alpha_2, \tag{16a,b}$$

$$b_{1p} = (e_{21}\beta_1^3 - \beta_1 p) = -e_{21}\beta_1\beta_2^2, \quad b_{2p} = (e_{21}\beta_2^3 + \beta_2 p) = -e_{21}\beta_1^2\beta_2. \tag{16c,d}$$

The final term in each of these equations is obtained by using one of equations (8a–d). For non-trivial solutions of equation (15), the determinant of the matrix must vanish. For computational purposes, its form can be simplified by dividing each of its columns by the top element in the column and then, by equating the simplified determinant to zero, one obtains

$$\begin{vmatrix} 1 & 1 & -1 & -1 \\ \alpha_1^2 & \alpha_2^2 & 0 & 0 \\ 0 & 0 & \beta_1^2 & \beta_2^2 \\ -\alpha_1\alpha_2^2 \tanh \alpha_1/2 & -\alpha_1^2\alpha_2 \tanh \alpha_2/2 & -\dfrac{\beta_1\beta_2^2}{e_{12}} \tanh \beta_1/2 & -\dfrac{\beta_1^2\beta_2}{e_{12}} \tanh \beta_2/2 \end{vmatrix} = 0. \quad (17)$$

This can be expanded to yield the frequency equation

$$\alpha_2^3 \tanh(\alpha_1/2) - \alpha_1^3 \tanh(\alpha_2/2) + X(p, \Omega)[\beta_2^3 \tanh(\beta_1/2) - \beta_1^3 \tanh(\beta_2/2)] = 0 \quad (18a)$$

in which

$$X(p, \Omega) = \frac{\sqrt{e_{21}\mu_{21}}\sqrt{(p/2)^2 + \Omega^2}}{\sqrt{(p/2e_{21})^2 + (\mu_{21}/e_{21})\Omega^2}}. \quad (18b)$$

When the beams are identical, $e_{21} = 1 = \mu_{21}$ and $X(p, \Omega) = 1$. The simple relationships which exist between the α's and β's ($\beta_2 = \mathrm{i}\alpha_1$, $\alpha_2 = \mathrm{i}\beta_1$) can now be used to recast equation (18a) into the much simpler form

$$\beta_1^3(\tanh \alpha_1/2 + \tan \alpha_1/2) + \alpha_1^3(\tanh \beta_1/2 + \tan \beta_1/2) = 0 \quad (\text{for } e_{21} = 1 = \mu_{21}). \quad (19)$$

3.2. BEAMS FIXED TOGETHER AT THEIR ENDS

The beams still vibrate in modes given by equations (9a) or (9b) but the boundary conditions are now

(1) equal displacements of the beams at each end:

$$w_1 = w_2 \quad \text{at } \xi = \pm 1/2, \quad (20a)$$

(2) equal gradients of the beams at each end:

$$\mathrm{d}w_1/\mathrm{d}\xi = \mathrm{d}w_2/\mathrm{d}\xi \quad \text{at } \xi = \pm 1/2, \quad (20b)$$

(3) zero total moment on the beams at each end:

$$EI_1(\mathrm{d}^2w_1/\mathrm{d}\xi^2) + EI_2(\mathrm{d}^2w_2/\mathrm{d}\xi^2) = 0 \quad \text{at } \xi = \pm 1/2,$$

i.e.,

$$\mathrm{d}^2w_1/\mathrm{d}\xi^2 + e_{21}(\mathrm{d}^2w_2/\mathrm{d}\xi^2) = 0 \quad \text{at } \xi = \pm 1/2, \quad (20c)$$

(4) zero combined transverse force in the beams at each end: the end gradients of the two beams are now equal and their axial loads are equal and opposite; the vertical components

of these loads at the ends therefore automatically cancel one another; the remaining transverse forces are the shear forces, $EI(\mathrm{d}^3w/\mathrm{d}x^3)$ in the beams, so

$$EI_1(\mathrm{d}^2w_1/\mathrm{d}\xi^3) + EI_2(\mathrm{d}^3w_2/\mathrm{d}\xi^3) = 0 \quad \text{at } \xi = \pm 1/2,$$

i.e.,

$$\mathrm{d}^2w_1/\mathrm{d}\xi^2 + e_{21}(\mathrm{d}^2w_2/\mathrm{d}\xi^2) = 0 \quad \text{at } \xi = \pm 1/2. \tag{20d}$$

These boundary conditions are all expressed by the single matrix equation

$$\begin{bmatrix} \cosh\alpha_1/2 & \cosh\alpha_2/2 & -\cosh\beta_1/2 & -\cosh\beta_2/2 \\ \alpha_1\sinh\alpha_1/2 & \alpha_2\sinh\alpha_2/2 & -\beta_1\sinh\beta_1/2 & -\beta_2\sinh\beta_2/2 \\ \alpha_1^2\cosh\alpha_1/2 & \alpha_2^2\cosh\alpha_2/2 & (\beta_1^2e_{21})\cosh\beta_1/2 & (\beta_2^2e_{21})\cosh\beta_2/2 \\ \alpha_1^3\sinh\alpha_1/2 & \alpha_2^3\sinh\alpha_2/2 & (\beta_1^3e_{21})\sinh\beta_1/2 & (\beta_2^3e_{21})\sinh\beta_2/2 \end{bmatrix} \begin{Bmatrix} A_1 \\ A_2 \\ B_1 \\ B_2 \end{Bmatrix} = 0. \tag{21}$$

Dividing each column of the 4×4 matrix by its top element, multiplying out the matrix determinant and equating it to zero, leads to the frequency equation for the pair of beams in the form

$$\begin{aligned}&(\beta_1^2+\alpha_1^2)^2[\tan\alpha_1/2\tanh\beta_1/2 + \tan\beta_1/2\tanh\alpha_1/2] \\ &\quad + (\beta_1^2+\alpha_1^2e_{21})(\beta_1^2e_{21}+\alpha_1^2)[\tan\alpha_1/2\tan\beta_1/2 + \tanh\alpha_1/2\tanh\beta_1/2] \\ &\quad + \beta_1\alpha_1(1-e_{21})2[\alpha_1^2\tan\alpha_1/2\tanh\alpha_1/2 + \beta_1^2\tan\beta_1/2\tanh\beta_1/2] = 0.\end{aligned} \tag{22}$$

This reduces to the surprisingly simpler form when the two beams are identical ($e_{21} = 1$):

$$(\tan\alpha_1/2 + \tanh\alpha_1/2)(\tan\beta_1/2 + \tanh\beta_1/2) = 0, \tag{23a}$$

so either

$$(\tan\alpha_1/2 + \tanh\alpha_1/2) = 0 \tag{23b}$$

or

$$(\tan\beta_1/2 + \tanh\beta_1/2) = 0. \tag{23c}$$

These frequency equations have exactly the same form as those for the symmetric modes of uniform fully fixed beams without any axial loads. The only difference lies in the definitions of α and β but this makes no difference to the numerical values of α_1 and β_1 which satisfy the equations and which are quoted in standard textbooks as 4·730, 10·996, 17·279, etc. Each of these is just one of a set of *four* roots. The other three in the set for 4·730 are $-4{\cdot}730$ and $\pm 4{\cdot}730\mathrm{i}$. $\alpha = 4{\cdot}730\mathrm{i}$ is found to satisfy equation (23b) for all values of p. Substituting this value into equation (5a) and solving it for Ω leads to

$$\Omega = 4{\cdot}730^2\sqrt{1 - \frac{p}{4{\cdot}730^2}} = 22{\cdot}373\sqrt{1 - \frac{p}{22{\cdot}373}} \quad (p \text{ +ve in compression}) \tag{24}$$

for the pair of beams with $e_{21} = 1 = \mu_{21}$. Obviously, one of the frequencies of this beam configuration vanishes when $p = 22{\cdot}373$. This value does not correspond to a static buckling load of one of the beams on its own, but its equality to the ND (= "non-dimensional") frequency of a fully fixed beam is noteworthy.

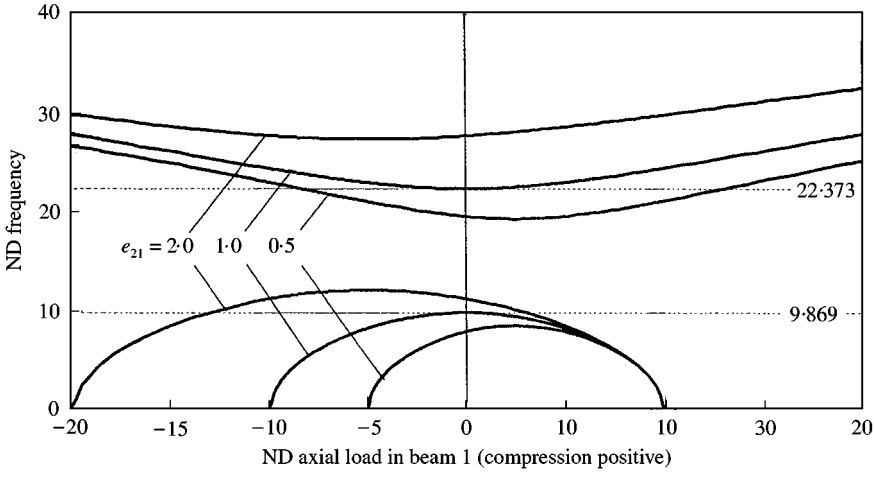

Figure 4. Natural frequencies versus ND axial load for the pinned pair of self-loaded beams at different values of the stiffness ratio.

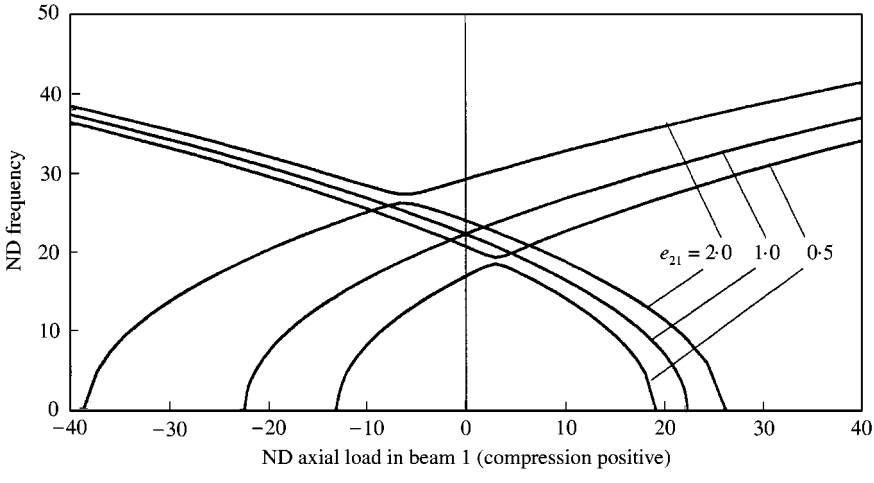

Figure 5. Natural frequencies versus ND axial load for the fixed pair of self-loaded beams at different values of the stiffness ratio.

3.3. COMPUTED FREQUENCIES AND MODES

3.3.1. *The frequencies*

Figures 4 and 5 show curves of the two lowest frequencies plotted against p for the paired beams with pinned ends (Figure 4) and fixed ends (Figure 5), the different curves on each figure relating to different values of e_{21}. The fundamental frequencies of the pinned pairs (i.e., the lower set of curves) all vanish for all values of e_{21} when the ND axial load in beam 1 is $+\pi^2$, i.e., when the self-load in beam 1 is equal to its own buckling load. The negative values of p at which the frequencies vanish correspond to the buckling load of beam 2 which increases, of course, as e_{21} increases. This critical p-value is $e_{21}\pi^2$. The minimum frequencies of any of the upper branch curves and the maximum frequencies of its corresponding lower branch curve occur at (or very close to) the value of p mid-way between the critical values at which the fundamental frequencies vanish.

There is a clear frequency gap between the sets of upper and lower curves of Figure 4. This is explained by considering firstly a pinned pair of identical beams ($e_{21} = 1$) with $p = 0$, i.e., without any axial load. These beams can vibrate identically but in anti-phase with one another, each in its sinusoidal mode of a pin-ended beam with zero displacement at each end. The ND frequency of this mode is π^2. The same beams can vibrate identically and in-phase with one another in the fundamental mode of a free–free beam at the ND frequency of 22·373. These two frequencies are precisely those indicated by the curves of Figure 4 for $e_{21} = 1$ and $p = 0$. As the value of p increases or decreases from $p = 0$, the frequencies follow the curves away from these values.

The curves for the pair of beams which are fixed together at their ends (Figure 5) show some of the same features as those of Figure 4. The fundamental frequencies vanish at critical values of p and their max/min values occur at (or very close to) values of p midway between the appropriate pairs of critical values. In this case, however, the critical values cannot be identified with the buckling loads of single beams fixed at their ends. When the two beams are identical ($e_{21} = 1$), the critical value of the ND parameter p is found (as shown above) to be exactly the same as the ND *frequency* of a single fixed or free beam, i.e., 22·373. This contrasts with the ND buckling load of $4\pi^2 = 39{\cdot}478$ for a single fully fixed beam.

It should be observed that the curves for $e_{21} = 1$ in Figure 5 actually cross over one another, whereas the upper and lower curves ($e_{21} = 2$ and 0·5) closely approach one another as p increases but then veer away as the min/max frequencies are passed. Although this is scarcely discernible in Figure 5, it has been verified by very detailed numerical examination.

Figures 4 and 5 suggest an answer to the initial question, "If the temperature of one part of a two-beam structure is raised, how do the natural frequencies of the whole structure change? Do they rise or fall?" Raising the temperature of one of the beams increases its axial compressive load while the other beam is stretched. If these loads are initially zero, the variation of the natural frequencies of a pair of beams is clear from the figures. If the two beams are pinned and identical ($e_{21} = 1$), the two frequencies at $p = 0$ are stationary with respect to p but a finite change of p (positive or negative) cause the fundamental frequency to drop and the frequency of the second symmetric mode to rise. If the pinned pair are dissimilar with beam 2 being less stiff than beam 1 (e.g., $e_{21} = 0{\cdot}5$) the stationary frequency is located at a positive value of p. From an initial value of $p = 0$, a positive increase of temperature and compressive load in beam 1 now causes the fundamental frequency to rise and the second mode frequency to drop. On the other hand, when beam 2 of the dissimilar pair is stiffer than beam 1 (say $e_{21} = 2$) the positive change of p from $p = 0$ causes the fundamental frequency to drop and the second mode frequency to rise, albeit very slightly.

Whether the frequency rises or falls with increasing p obviously depends on the p-wise location of the maximum and minimum frequencies on the frequency versus p-curves. For each curve, these max/min values occur at p-values very close to (if not exactly at) the average of the two critical p-values which cause the fundamental frequency to vanish. One can therefore conclude that the fundamental frequency will rise and the second mode frequency will fall if the average of the two critical p-values is positive. The reverse is true if the average is negative. Consideration of Figure 5 shows the same principle to apply to the fixed-beam pairs.

For a pinned beam-pair, each pair of critical values is found from the well-known Euler buckling load for pin-ended beams but for the fixed pair of beams they are not so readily determined. The beams are only fixed at their ends relative to one another and not in an absolute sense. However, the methods of static buckling analysis can still be applied to find the critical loads.

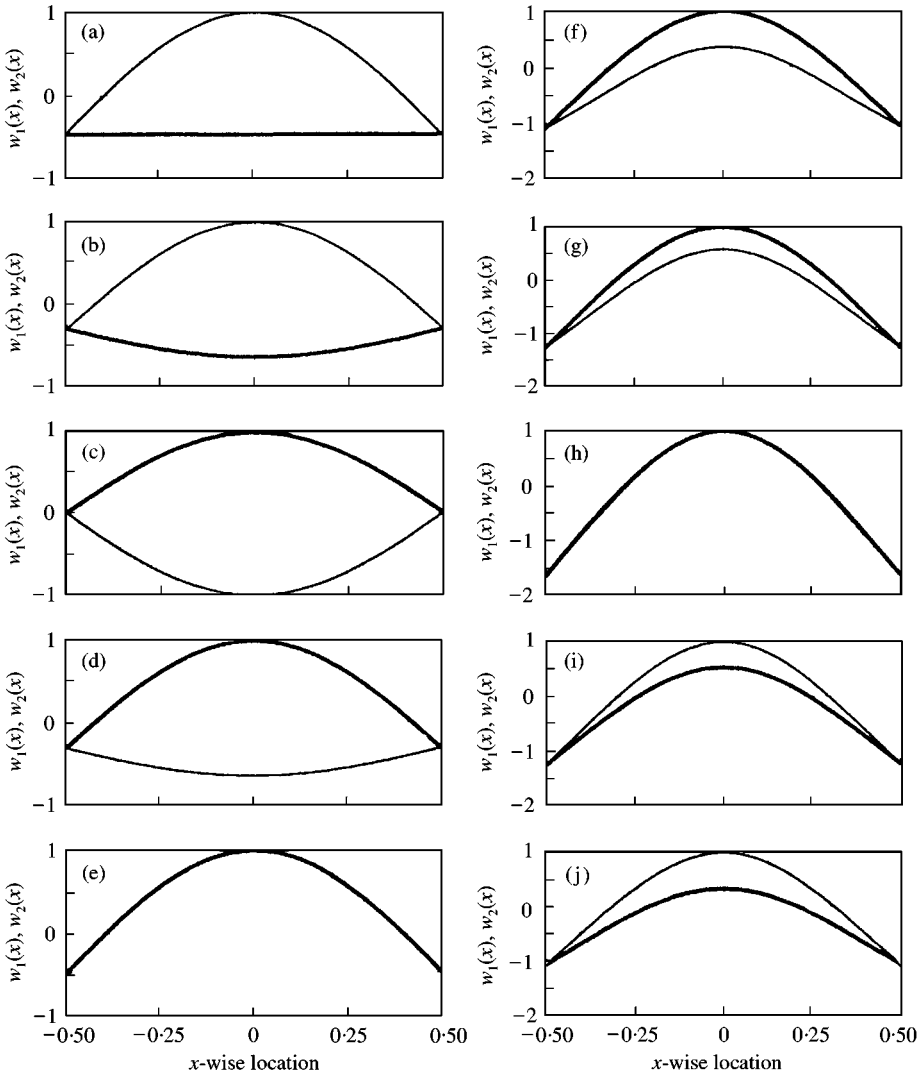

Figure 6. Some flexural modes of the pinned beam-pairs; $e_{21} = 0{\cdot}5$: (a) $p = -4{\cdot}93$; ND freq. = 0·282; (b) $p = -1{\cdot}21$; ND freq. = 7·958; (c) $p = 2{\cdot}37$; ND freq. = 8·546; (d) $p = +6{\cdot}19$; ND freq. = 7·188; (e) $p = +9{\cdot}85$; ND freq. = 0·2823; (f) $p = -4{\cdot}93$; ND freq. = 21·065; (g) $p = -1{\cdot}21$; ND freq. = 19·58; (h) $p = +2{\cdot}37$; ND freq. = 19·348; (i) $p = +6{\cdot}19$; ND freq. = 19·89; (j) $p = +9{\cdot}85$; ND freq. = 21·11.

3.3.2. *The modes*

Computed non-dimensional flexural modes of the beams are shown in Figures 6 and 7 for the pinned pairs and Figure 8 for the fixed pairs. Figure 6 relates to pairs of different beams ($e_{21} = 2, m_{21} = 1$) and Figure 7 to identical beams ($e_{21} = 1, m_{21} = 1$). Diagrams in the left-hand columns of each figure show the fundamental modes and the right-hand columns show the next higher modes. Successive diagrams in each column show how the modes vary as p changes from the lower (negative) critical value through to the higher (positive) critical value. They include the p-values yielding the max/min frequencies for the given e_{21}'s and two p-values lying mid-way between these and the critical values.

When the beam pairs, pinned or fixed, vibrate in the modes of the fundamental frequencies of Figures 4 and 5 the beams vibrate in anti-phase with one another, irrespective

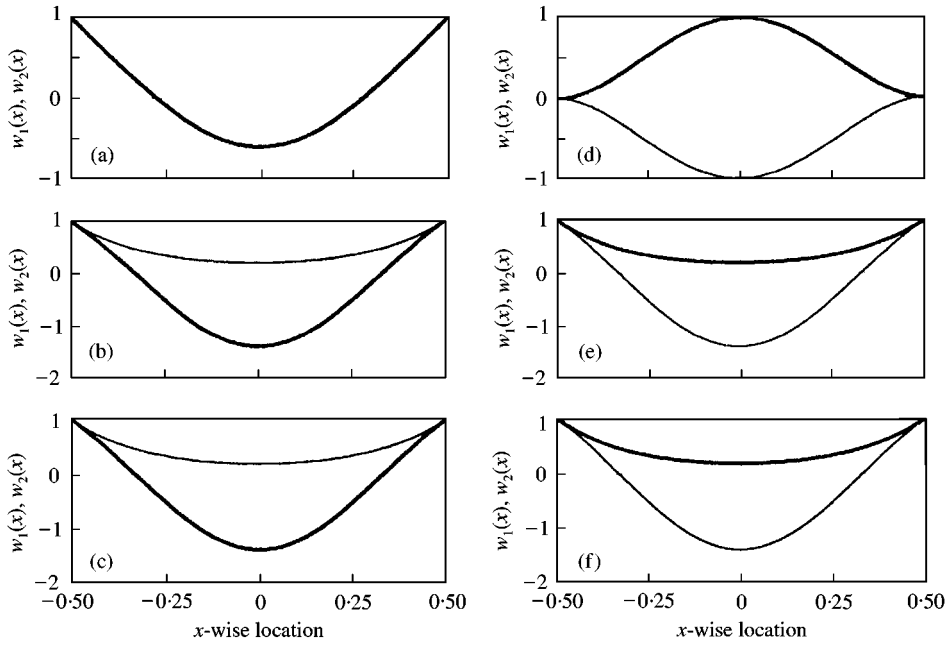

Figure 7. Some flexural modes of the fixed beam-pairs; $e_{21} = 1$: (a) $p = 0$; freq. = 22·373; (b) $p = +11{\cdot}07$; freq. = 15·89; (c) $p = +22{\cdot}33$; freq. = 1·01; (d) $p = 0$; freq. = 22·373; (e) $p = +11{\cdot}07$; freq. = 27·36; (f) $p = +22{\cdot}33$; freq. = 31·62.

of the end conditions, with the amplitude of the compressed beam (i.e., beam 1 when p is positive, beam 2 when p is negative) exceeding that of the stretched beam. The reverse is true when they vibrate in the modes of the upper branches of Figures 4 and 5 for then they vibrate in phase with one another and the compressed beam has the lower amplitude. These features are true for all values of e_{21} except at the value of p for a frequency maximum or minimum when the amplitudes of the two beams are either exactly or very nearly equal.

The progressive change of the mode as p increases from the negative to the positive critical values is clearly apparent. Further calculations with other values of e_{21} suggest that the general form of the mode does not depend upon the value of e_{21} although small differences do exist in the precise forms.

The modes of two identical beams fixed together at their ends ($e_{21} = 1$) are particularly interesting as they are actually independent of the value of p except for $p = 0$. This fact has been proved analytically as well as numerically. Accordingly, the modes for $e_{21} = 1$ shown in Figure 7 relate only to $p = 0$ and two positive p-values. The modes for negative p-values are the same except for an interchange of the curves for beams 1 and 2. The modes for $p = 0$ appear to be different from those for $e_{21} \neq 0$ but as already explained they are degenerate modes. As such they can be combined in any proportion to form other legitimate normal modes and in appropriate proportions can be combined exactly into the same modes as those for $e_{21} \neq 0$.

3.4. THE EFFECTS OF DIFFERENT VIBRATION AMPLITUDES IN THE TWO BEAMS

A potential analytical problem is suggested when one considers the modes for the pinned beams when p is close to a critical value. At this condition (see Figure 6) the stretched beam

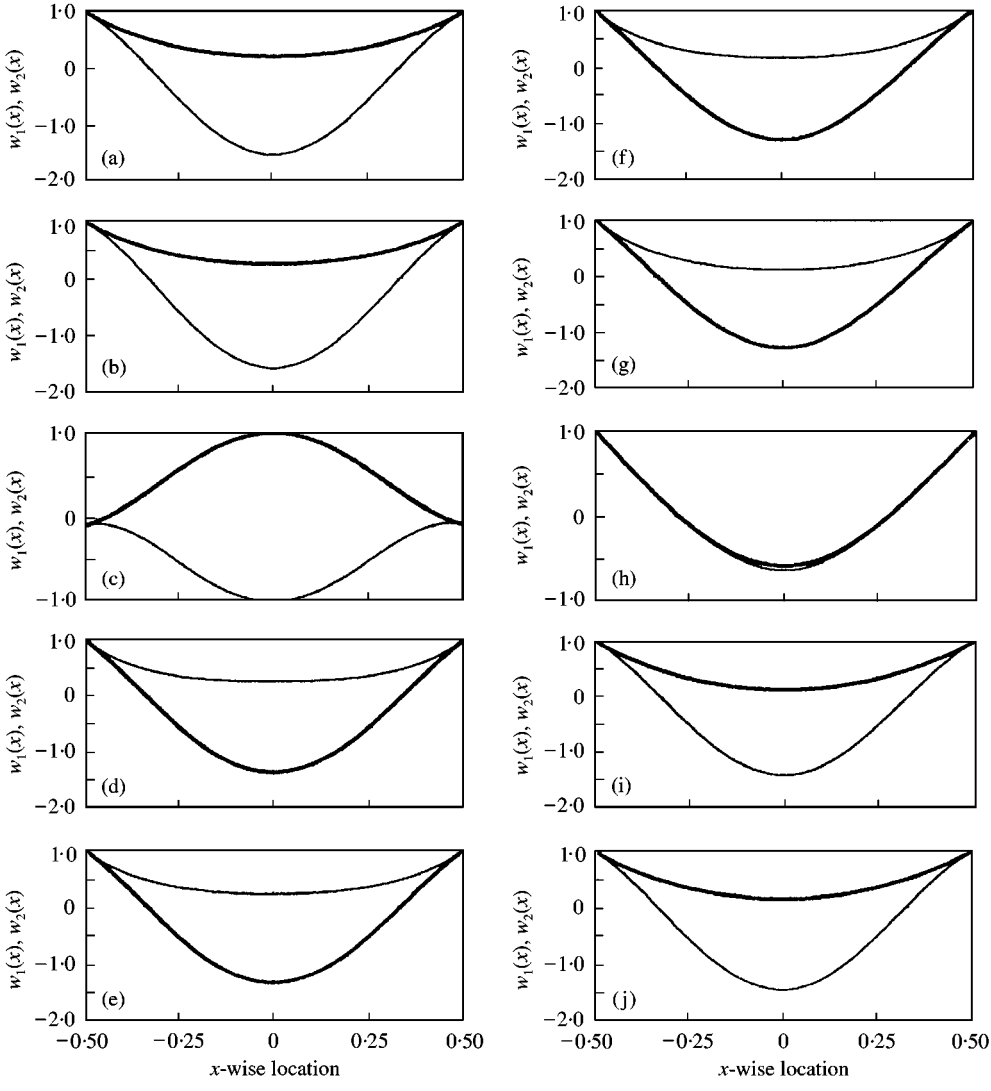

Figure 8. Some flexural modes of the fixed beam-pairs; $e_{21} = 0{\cdot}5$: (a) $p = -12{\cdot}8$; freq. = 2·03; (b) $p = -4{\cdot}55$; freq. = 13·76; (c) $p = +3{\cdot}104$; freq. = 18·60; (d) $p = +11{\cdot}09$; freq. = 13·43; (e) $p = +19{\cdot}15$; freq. = 0·262; (f) $p = -12{\cdot}8$; freq. = 26·77; (g) $p = -4{\cdot}55$; freq. = 23·06; (h) $p = +3{\cdot}104$; freq. = 19·367; (i) $p = +11{\cdot}09$; freq. = 23·25; (j) $p = +19{\cdot}15$; freq. = 26·84.

vibrates almost as a rigid body, remaining straight, while the compressed beam bends and vibrates in a half-sine mode superimposed upon it. The exaggerated vertical scale of these diagrams shows that the bent beam must be longer around its curved mid-surface than the unbent stretched beam. However, the straight distances between their pinned ends must always be equal although they may vary throughout the vibration cycle. Since the beams are of equal length when they are unbent, equal straight distances between their ends can only be maintained when they bend provided internal time-varying axial forces are developed which stretch one beam and compress the other. These "perturbing" forces can only exist in the form of an equal and opposite self-balancing pair. If their magnitudes are significant compared with the initial self-straining pair P within the system, the P-term in

equations (1) and (2) and the non-dimensional p in all subsequent equations become significantly time-dependent. The whole system then changes from being linear to non-linear, so it is pertinent to examine the required magnitude of the perturbing pair as a function of P and the vibration amplitude. To do this one proceeds as follows.

The (straight) distance between the ends of a beam of length/when it bends in the mode $w(x)$ is $l - \frac{1}{2}\int_{-l/2}^{+l/2} (\mathrm{d}w/\mathrm{d}x)^2 \,\mathrm{d}x$. In general, this is different for the two beams in question, the difference between them being $\delta u_{bending} = \frac{1}{2}\int_{-l/2}^{+l/2} \lceil (\mathrm{d}w_1/\mathrm{d}x)^2 - (\mathrm{d}w_2/\mathrm{d}x)^2 \rceil \mathrm{d}x$. When the two beams are subjected to the perturbing pair of axial forces $\pm\delta P(t)$, the resulting relative change of length between them is $\delta u_{P(t)} = \delta P(t) \lceil (1/E_1A_1) + (1/E_2A_2) \rceil l$. This must be equal and opposite to $\delta u_{bending}$, from which one finds $\delta P/P = (I_{12}/2p) [w_{max}/\kappa]^2$. w_{max} is the actual vibration amplitude at the centre of the compressed beam and κ is the radius of gyration of the beam cross-section, I_{12} is a non-dimensional value of $\delta u_{bending}$ in which the integrals are evaluated from normalized modes w_1 and w_2 having unit value at the centre of the compressed beam.

The greatest value of I_{12} is 2·655 when the beams are pinned, $e_{21} = 1$ and p is close or equal to the critical value of π^2. This worst case yields $\delta P/P = 0{\cdot}1345\ [w_{max}/\kappa]^2$ and shows that w_{max} must have a value approaching κ before the perturbing force becomes significant compared with P. This would be quite a large displacement, so the linear assumptions made in this paper are justifiable for small and moderate vibration amplitudes.

An exact non-linear solution to a similar (though simpler) problem was investigated by Woinowsky-Krieger [12] who considered a simply supported beam rigidly restrained against axial displacement at its ends. Full allowance was made for the varying tension load in the beam as it deflected which would be superimposed upon any steady axial load, tensile or compressive. The exact time dependence of free vibration was found in terms of elliptic functions, and calculations showed the frequency to increase by 0·08% when $w_{max}/\kappa = 0{\cdot}1$ and by 8·9% when $w_{max}/\kappa = 1{\cdot}0$. These percentages would be smaller for the two-beam model which has been studied in this paper as neither beam is rigidly restrained against axial displacement at its ends. The restraint from each beam on the other is elastic, not rigid.

4. SIMPLE REDUNDANT FRAMES

4.1. GENERAL EQUATIONS

Figure 9 illustrates a redundant six-beam frame. Internal loads are generated in such a structure if any member is initially too short or too long or if a non-uniform temperature field causes unequal thermal strains in the members. For simplicity of analysis, the frame will be considered to be doubly symmetrical so that the two diagonal members are identical in size, stiffness and mass, as also are the opposite pairs of side members. Again for simplicity, only symmetrical modes of vibration will be studied. The diagonal members can therefore both be identified as beam 1, the top and bottom members as beam 2 and the left- and right-hand members as beam 3.

The equations of flexural motion and the wave numbers for the beams have the same forms as equations (4a,b) and (5a,b) but the three beams now have different axial loads denoted by P_1, P_2 and P_3 where $P_2 = -P_1 \cos\theta_2 = -P_1 (l_2/l_1)$, $P_3 = -P_1 \cos\theta_3 = -P_1 (l_3/l_1)$. We introduce the non-dimensional length ξ, the axial load parameter p and the non-dimensional frequency Ω, all based on the length, load, stiffness and mass of the diagonal member so $\xi = x/l_1$, $p = Pl_1^2/EI_1$, $\Omega^2 = (m_1 l_1^4/EI_1)\,\omega^2$. The stiffness and mass ratios of beams 2 and 3 are defined as before by $e_{21} = EI_2/EI_1$, $\mu_{21} = m_2/m_1$, $e_{31} = EI_3/EI_1$, $\mu_{31} = m_3/m_1$. It follows that the non-dimensional equation of

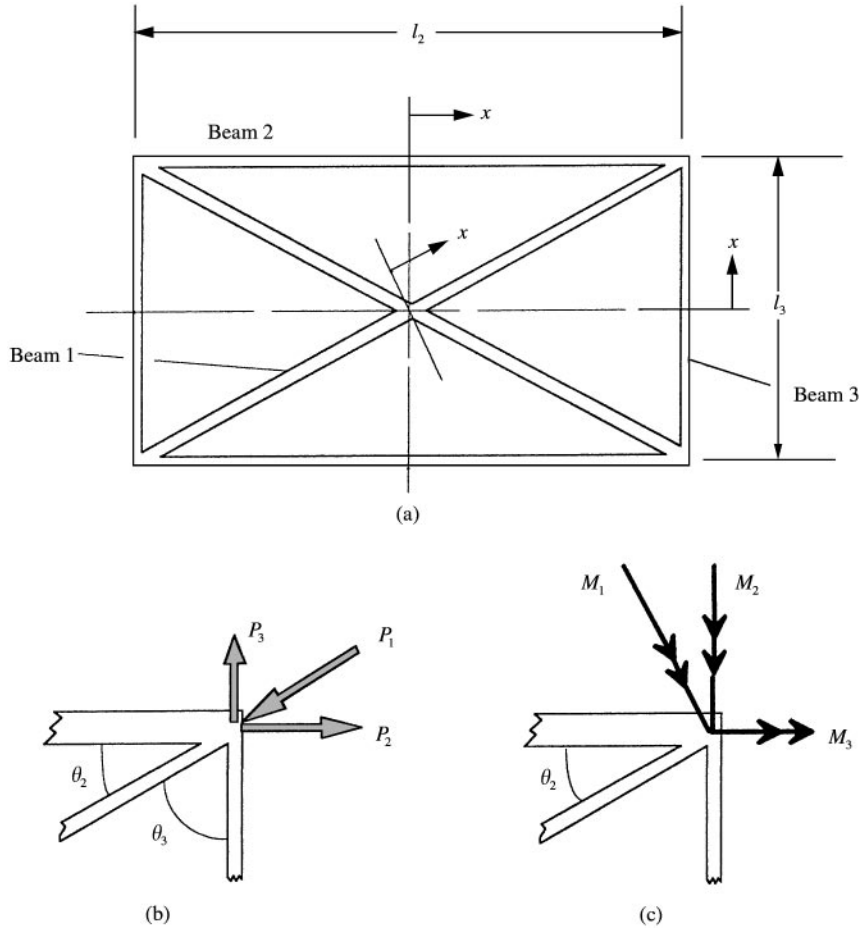

Figure 9. The six-beam frame: (a) the overall schematic diagram, dimensions and co-ordinate system; (b) the interacting axial forces at a joint; (c) the interacting bending moments at a joint.

free vibration for beam 1 is the same as equations (4a) while the equations for beams 2 and 3 are

$$\frac{\mathrm{d}^4 w_2}{\mathrm{d}\xi^4} - p\cos\theta_2 \frac{1}{e_{21}} \frac{\mathrm{d}^2 w_2}{\mathrm{d}\xi^2} - \frac{\mu_{21}}{e_{21}} \Omega^2 w_2 = 0, \tag{4c}$$

$$\frac{\mathrm{d}^4 w_3}{\mathrm{d}\xi^4} - p\cos\theta_3 \frac{1}{e_{31}} \frac{\mathrm{d}^2 w_3}{\mathrm{d}\xi^2} - \frac{\mu_{31}}{e_{31}} \Omega^2 w_3 = 0. \tag{4d}$$

These have the same form of solution as for beam 1 so $w_2 = B\exp\beta\xi$, $w_3 = C\exp\gamma\xi$, and the wave numbers β and γ are given by

$$\beta^4 - p\cos\theta_2 \frac{1}{e_{21}} \beta^2 - \frac{\mu_{21}}{e_{21}} \Omega^2 = 0, \tag{5c}$$

$$\gamma^4 - p\cos\theta_3 \frac{1}{e_{31}} \gamma^2 - \frac{\mu_{31}}{e_{31}} \Omega^2 = 0, \tag{5d}$$

of which the solutions are

$$\beta_1 = \pm\sqrt{\frac{p}{2}\frac{\cos\theta_2}{e_{21}} + \sqrt{\left(\frac{p}{2}\frac{\cos\theta_2}{e_{21}}\right)^2 + \frac{\mu_{21}}{e_{21}}\Omega^2}}, \tag{7c}$$

$$\beta_2 = \pm\sqrt{\frac{p}{2}\frac{\cos\theta_2}{e_{21}} + \sqrt{\left(\frac{p}{2}\frac{\cos\theta_2}{e_{21}}\right)^2 + \frac{\mu_{21}}{e2^1}\Omega^2}}, \tag{7d}$$

$$\gamma_1 = \pm\sqrt{\frac{p}{2}\frac{\cos\theta_3}{e_{31}} + \sqrt{\left(\frac{p}{2}\frac{\cos\theta_3}{e_{31}}\right)^2 + \frac{\mu_{31}}{e_{31}}\Omega^2}} \tag{7e}$$

and

$$\gamma_2 = \pm\sqrt{\frac{p}{2}\frac{\cos\theta_3}{e_{31}} - \sqrt{\left(\frac{p}{2}\frac{\cos\theta_3}{e_{31}}\right)^2 + \frac{\mu_{31}}{e_{31}}\Omega^2}}. \tag{7f}$$

The symmetric modes of vibration of beam 2 are still expressible in the hyperbolic form of equation (9b). Those of beam 3 are expressible likewise by

$$w_3 = C_1\cosh\gamma_1\xi + C_2\cosh\gamma_2\xi. \tag{9c}$$

The symmetric modes of vibration of the whole six-beam frame are therefore defined by six hyperbolic functions and the six coefficients A_1, A_2, B_1, B_2, C_1, C_2 which together must satisfy the geometric and natural (equilibrium) boundary conditions at the corners of the frame. By virtue of the symmetry of the frame, satisfying these conditions at just one corner automatically satisfies them at the other corners.

4.2. THE BOUNDARY CONDITIONS AND FREQUENCY EQUATION FOR THE SIX-BEAM FRAME WITH PINNED JOINTS

Consider firstly a pin-jointed frame. At the top right-hand corner (where $\xi = 1/2$ for beam 1, $\xi = l_{21}/2$ for beam 2 and $\xi = l_{31}/2$ for beam 3), equality of the beam flexural displacements requires that

$$w_1(1/2) = w_2(l_{21}/2) \quad \text{and} \quad w_1(1/2) = w_3(l_{31}/2). \tag{25a,b}$$

Since the joints are pinned, the bending moment in each beam at the corner is zero so

$$\frac{\mathrm{d}^2w_1}{\mathrm{d}\xi^2} = 0 \quad \text{at } \xi = \frac{1}{2}, \quad \frac{\mathrm{d}^2w_2}{\mathrm{d}\xi^2} = 0 \quad \text{at } \xi = \frac{l_{21}}{2}, \quad \frac{\mathrm{d}^2w_3}{\mathrm{d}\xi^2} = 0 \quad \text{at } \xi = \frac{l_{31}}{2}. \tag{26a–c}$$

The total transverse force in the three beams at a corner must also be zero. In the same way as for the simple pair of joined beams, this must include the shear forces in the beams, EIw''', and the vertical components of the axial forces, Pw'. Hence,

$$\left|EI_1\frac{\mathrm{d}^3w_1}{\mathrm{d}x^3} + P\frac{\mathrm{d}w_1}{\mathrm{d}x}\right|_{x=l_1/2} + \left|EI_2\frac{\mathrm{d}^3w_2}{\mathrm{d}x^3} - P\cos\theta_2\frac{\mathrm{d}w_2}{\mathrm{d}x}\right|_{x=l_2/2}$$

$$+ \left|EI_3\frac{\mathrm{d}^3w_3}{\mathrm{d}x^3} - P\cos\theta_3\frac{\mathrm{d}w_3}{\mathrm{d}x}\right|_{x=l_3/2} = 0.$$

Expressing this in non-dimensional form by dividing by EI_1/l^3 and introducing the non-dimensional parameters yield

$$\left|\frac{d^3w_1}{d\xi^3} + p\frac{dw_1}{d\xi}\right|_{\xi=1/2} + \left|e_{21}\frac{d^3w_2}{d\xi^3} - p\cos\theta_2\frac{dw_2}{d\xi}\right|_{\xi=l_{21}/2} + \left|e_{31}\frac{d^3w_3}{d\xi^3} - p\cos\theta_3\frac{dw_3}{d\xi}\right|_{\xi=l_{31}/2} = 0. \tag{27}$$

Next, substitute the expressions for $w_1(\xi)$, $w_2(\xi)$, $w_3(\xi)$ into the six equations (25a,b), (26a–c), (27) to yield six homogenous equations for the six A, B, C coefficients. The terms of these equations are listed in Appendix A. The natural frequencies of the frame are those frequencies at which the determinant of the matrix of these terms vanishes.

4.3. THE BOUNDARY CONDITIONS AND FREQUENCY EQUATION FOR THE SIX-BEAM FRAME WITH FIXED JOINTS

Now consider the frame in which the ends of the members are fixed to one another. The transverse displacements of the beams at their ends are again equal so

$$w_1(1/2) = w_2(l_{21}/2) \quad \text{and} \quad w_1(1/2) = w_3(l_{31}/2). \tag{28a,b}$$

The flexural gradients of the deflected beams which are fixed together at their ends are related in the following way. When the end of beam 2 is rotated through its gradient w_2', beam 1 undergoes the flexural rotation $w_2'\cos\theta_2$ at its end. At the same time, beam 3 undergoes a torsional rotation which, in general, will generate a torsional moment in beam 3. All such torsional moments will be neglected in this paper, it being assumed that the dynamic torsional stiffnesses of the beams are negligible compared with the dynamic bending stiffnesses. When the end of beam 3 is rotated through its gradient w_3', beam 1 undergoes the flexural rotation $w_3'\cos\theta_2$ so its total flexural rotation is given by $(dw_1/dx) = \cos\theta_2(dw_2/dx) + \cos\theta_3(dw_3/dx)$. Hence,

$$\left|\frac{dw_1}{d\xi}\right|_{\xi=1/2} - \cos\theta_2\left|\frac{dw_2}{d\xi}\right|_{\xi=l_{21}/2} - \cos\theta_3\left|\frac{dw_3}{d\xi}\right|_{\xi=l_{31}/2} = 0. \tag{29}$$

This is the appropriate "gradient-compatibility" boundary condition for the three beams fixed to one another at their common ends.

The bending moments at the ends of the three intersecting beams (M_1, M_2, M_3) are no longer zero but must, of course, be in equilibrium. By resolving these moments in the directions of the bending moment vectors in beams 2 and 3 one obtains, respectively, $M_1\cos\theta_2 + M_2 = 0$ and $M_2\cos\theta_3 + M_3 = 0$. These yield the following ND boundary condition equations:

$$\cos\theta_2|d^2w_1/d\xi^2|_{\xi=1/2} + e_{21}|d^2w_2/d\xi^2|_{\xi=l_{21}/2} = 0 \tag{30a}$$

and

$$\cos\theta_3|d^2w_1/d\xi^2|_{\xi=1/2} + e_{31}|d^2w_3/d\xi^2|_{\xi=l_{31}/2} = 0. \tag{30b}$$

The total transverse force in the three beams at a corner must again be zero. Since $P_2 = P_1\cos\theta_2$ and $P_3 = P_1\cos\theta_3$ and the beam gradients are related by equations (29a,b),

the sum of the vertical components of the axial loads at the ends of the beams is found to vanish identically. The total transverse force is then the simple sum of the shear forces in the beams so at a corner

$$EI_1(\mathrm{d}^3w_1/\mathrm{d}x^3) + EI_2(\mathrm{d}^3w_2/\mathrm{d}x^3) + EI_1(\mathrm{d}^3w_2/\mathrm{d}x^3) = 0$$

or in non-dimensional terms

$$|\mathrm{d}^3w_1/\mathrm{d}\xi^3|_{\xi=1/2} + e_{21}|\mathrm{d}^3w_2/\mathrm{d}\xi^3|_{\xi=l_{21}/2} + e_{31}|\mathrm{d}^3w_3/\mathrm{d}\xi^3|_{\xi=l_{31}/2} = 0. \tag{31}$$

Substituting the expressions for $w_1(\xi)$, $w_2(\xi)$, $w_3(\xi)$ into the six equations (28)–(30) yield six homogenous equations for the six A, B, C coefficients for the fixed-jointed frame. The terms of these equations are listed in Appendix A.

The six equations can be reduced to four if the frame is square and the side members have the same flexural stiffnesses and masses. The side members then all vibrate identically if the modes are symmetrical. Appendix A gives the terms of the corresponding 4×4 matrix equation and these are used in the calculations to be described.

It should be pointed out at this stage that determinental frequency equations of order lower than 6 or 4 as in Appendix A can be set up by using the dynamic stiffness method rather than the above method. For symmetrical frames and modes one then obtains a 4×4 equation for the pin-jointed frame and a 3×3 equation for the fixed-jointed frame. This is true whether the frames are square or rectangular, and whether or not the adjacent side members are identical.

4.4. COMPUTED FREQUENCIES AND MODES FOR THE SIX-BEAM FRAMES

4.4.1. *The frequencies*

Figures 10(a,b) and 11 show the natural frequencies of the symmetric modes of a six-beam frame plotted against the ND load in the diagonal members. Figures 10(a,b) relate to a frame with pinned joints and Figure 11 to one with fixed joints. In each case, the frames are square so $l_{21} = l_{31} = 1/\sqrt{2}$. The stiffness and mass ratios of the side members have been taken to be $e_{21} = e_{31} = 2$ and $m_{21} = m_{31} = 1$.

The way in which the frame frequencies vary with p follows the same general pattern as those of the pairs of beams shown in Figures 4 and 5. Fundamental frequencies fall to zero when the compression load in any one of the members approaches the critical buckling load of the member and is seen most clearly in Figure 10(a) for the pin-jointed frame. From simple static analysis we know the ND buckling load of the pinned diagonal members of this frame to be $p = +\pi^2$ while the side members buckle at $p = -55{\cdot}83$ $(= -\pi^2 e_{21}/l_{21}^2 \cos\theta_2)$. At both of these values the frequency is seen to vanish.

The large difference in the absolute values of these two critical p-value means that the curve for the fundamental frequencies is far from symmetrical about the frequency axis ($p = 0$). As a result, the fundamental frequency drops as the compressive load in the diagonal member increases from zero. On the other hand, the frequencies shown by the upper curve of Figure 10(a) (corresponding to the second symmetric frame mode) increase as p increases from zero. In order to verify the validity of this observation, frequency curves are shown in Figure 10(b) for a much wider range of diagonal compressive loads and frequencies.† The figure shows that the frequencies of each higher mode undulate with

†The extended p-range is, of course, quite impracticable as the structure becomes statically unstable outside the narrow range $-55{\cdot}48 < p < 9{\cdot}87$. Nevertheless, the extended range can be studied in principle even though not realizable in practice.

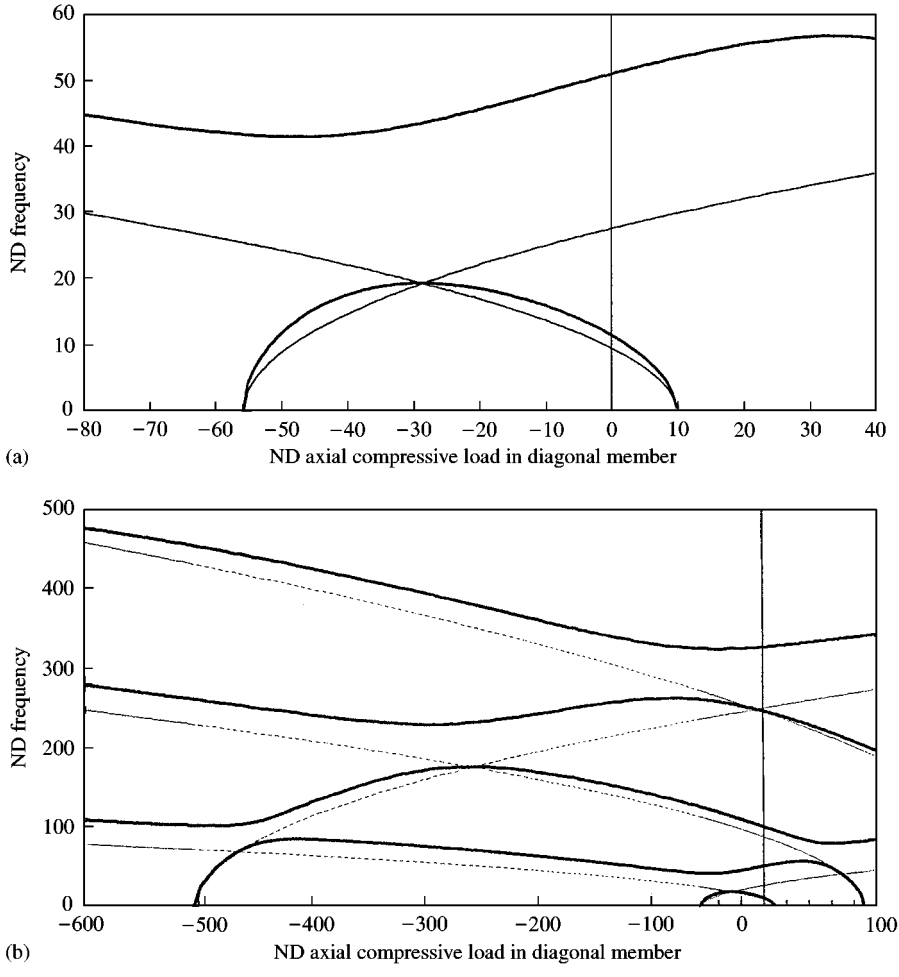

Figure 10. (a) Natural frequencies of the six-beam frame with pinned joints versus ND axial load in the diagonal member; $l_{21} = l_{31} = 1$; $e_{21} = e_{31} = 2$; $m_{21} = m_{31} = 1$; restricted axial load range. ————, frame frequencies; ——, frequencies of beams 1 and 2 when axially loaded, independent and simply supported. (b) Natural frequencies of the square six-beam frame with pinned joints versus ND axial load in the diagonal member; component parameters as for Figure 10(a); extended axial load range ——, frame frequencies; ----------, frequencies of beams 1 and 2 when axially loaded, independent and simply supported.

varying p before they finally descend to zero at high order ND buckling loads. Whether the frequency increases or decreases with p at $p = 0$ clearly depends on the location of $p = 0$ along the undulating curve.

Figure 10(b) has frequency curves superimposed upon it for two independent simply supported beams under axial load, one having the length and flexural properties of the diagonal member and the other having the length and properties of a side member. This set of curves forms a "curved grid" (if they are not actual asymptotes) between which the frequency curves for the framework are seen to fit. Notice that pairs of these independent-beam curves always intersect on the framework frequency curves. The lowest pair intersect at (or very close to) the maximum value of the fundamental frequency which occurs very close to $p = -28{\cdot}6$, (see Figure 10(a)). The proximity of the framework frequency curves to the independent-beam curves helps to explain the variation of the framework frequencies at $p = 0$.

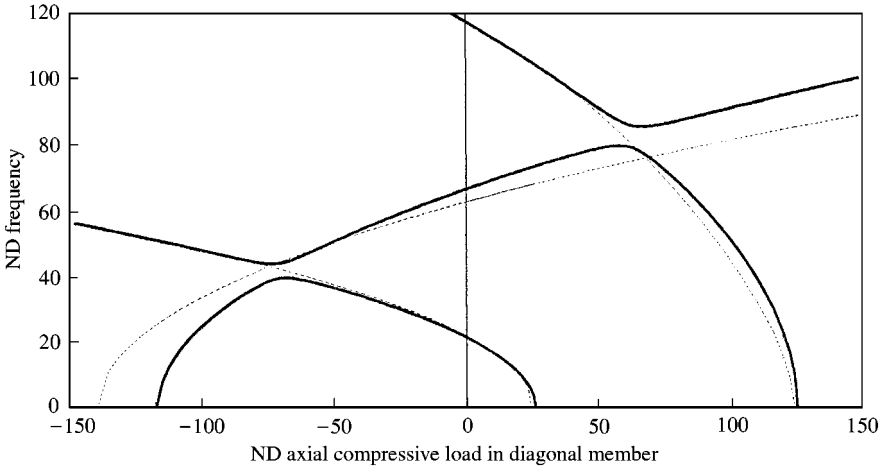

Figure 11. Natural frequencies of the square six-beam frame with fixed joints versus ND axial load in the diagonal member; $l_{21} = l_{31} = 1$; $e_{21} = e_{31} = 2$; $m_{21} = m_{31} = 1$; ——, frame frequencies; ---------, "mean frequencies" (as defined in text) of independent beams 1 and 2 when axially loaded and independent.

The frequencies shown in Figure 10(a) demonstrate another feature similar to that of the pinned pair of beams of Figure 4. There is a distinct gap between the frequencies of the fundamental mode (which are all less than $\Omega = 20$) and those of the curve above it which all exceed $\Omega = 40$ and belong to the second symmetric mode. This gap is much reduced when the joints of the frame are fixed instead of pinned, as seen on the curves for the fixed-jointed frame in Figure 11. As the axial load approaches $p = -70$, the frequencies of the fundamental and second symmetric modes (the lowest curve and the curve just above it) approach one another quite closely but then veer away. Recall that the same phenomenon was observed for the frequencies of the fixed pair of beams in Figure 5.

The values of p which cause the fundamental frequencies of the fixed-jointed frame to vanish are approximately 2·2 times those for the pinned frame. This compares with the similar feature for the fixed and pinned beam pairs.

Figure 11 shows that as the compression load in the diagonal members increases from zero the fundamental frequency of the fixed frame decreases like that of the pinned frame. The frequency of the second symmetric mode increases while the frequency of the third symmetric mode (the next curve up) decreases and at a greater rate than that of the fundamental. It then levels off and rises. The general shape of these curves is determined (as for the curves of the pinned frame) by a "curved grid" of frequency curves for independent axially loaded beams. Such curves are shown superimposed upon Figure 11. Now the independent beams considered for comparison with the pin-jointed frame had precisely defined simply supported boundary conditions so their p–Ω curves were easily determined. The boundary conditions for the independent beams for comparison with the fixed-jointed frame are by no means simple. The so-called "fixed" frame joints only fix the beams relative to one another so the fixing is not absolute. The actual boundary condition for any of the three intersecting beams is neither fully fixed nor simply supported but is somewhere between the two and is actually a function of frequency. Accordingly, the independent beam frequency curves shown in Figure 11 have been chosen to lie between those of fully fixed and simply supported independent beams. The mean has been chosen arbitrarily to lie mid-way between the corresponding pairs of p at a given frequency, not mid-way between the two

frequencies at a given p. These curves clearly map out p–Ω zones within which the actual frame frequency curves are more-or-less contained. In view of the arbitrary choice for the mean curves, it is fortuitous that some of them lie so close to the curves for the frame, especially at two of the zero frequencies.

It was not practicable (nor is it really necessary) to extend the p-range of Figure 11 to the same extent as that of Figure 10(b). Increasing difficulty was encountered in the automatic computing process used to find the frequencies in an extended range. An iterative method was used which found the roots of the frequency determinant. Applied to the fixed frame it refused to converge in the extended range and even within the narrow range covered in Figure 10 ($-150 < p < 150$), convergence was only achieved when the starting values for the iteration had been chosen with great care. The same iterative method used for the pin-jointed frame gave no trouble and always converged satisfactorily, even over the whole extended range of p.

From Figures 10(a,b) and 11, it is evident that increasing the compressive load in the diagonal member from $p = 0$ has the same effect on the frame frequencies as did an increasing compressive load on the beam frequencies (Figures 6–8). Figures 10(a,b) and 11 apply to a frame with side members which are stiff compared with the diagonal members. The average of the pairs of critical p-values for zero fundamental frequency is seen to be negative on each of these figures. As the maxima and minima on the frequency curves always occur close to these average values, the fundamental frequencies drop as p increases from zero while the frequencies of the second modes rise. An increase in diagonal compression from $p = 0$ therefore causes the fundamental frequencies to drop and the second mode frequencies to rise. Higher mode frequencies may rise or fall. If the side members are less stiff than the diagonal members such that their critical loads are less, this phenomenon would be reversed.

4.4.2. *The modes*

Modes of vibration of the frames are shown in Figure 12 corresponding to some of the points on the fundamental frequency curve of Figures 10(a) and 11. The mode of the diagonal member is indicated by a long curve and that of a side member by a short curve. Since symmetric modes only are being studied, all the side members vibrate identically and in phase with one another. The left-hand set of curves is for frames with pinned joints and the right-hand set is for fixed joints. From the top to the bottom diagram in each set, the value of p changes progressively from close to the negative critical value of p to close to the positive critical value. The corresponding frequencies at each extreme are therefore close to zero. The middle diagram corresponds to the p-value which yields the maximum fundamental frequency.

The modes of the pin-jointed frame (Figures 12(a)–12(e)) display features which are similar to those of the pinned pair of beams (Figure 6) in that when p is close to a critical value, the nearly buckled diagonal beam has a large flexural displacement while the other (side) beam is almost straight. On the other hand, the mode at a maximum fundamental frequency has comparable maximum distortional displacements in both beams.

Likewise, the modes of the fixed-jointed frame show similar features to those of the fixed pair of beams (Figures 12(f)–12(j)). When one of the beams is almost buckled ($p = -116{\cdot}6$ or $26{\cdot}101$) the unbuckled beam is no longer straight, being constrained to bend by virtue of its fixed connection to the deflected buckled beam. Observe, however, the nature of the diagonal beam deflection when the short side beams are under compression and buckled. This deflection decays rapidly from the

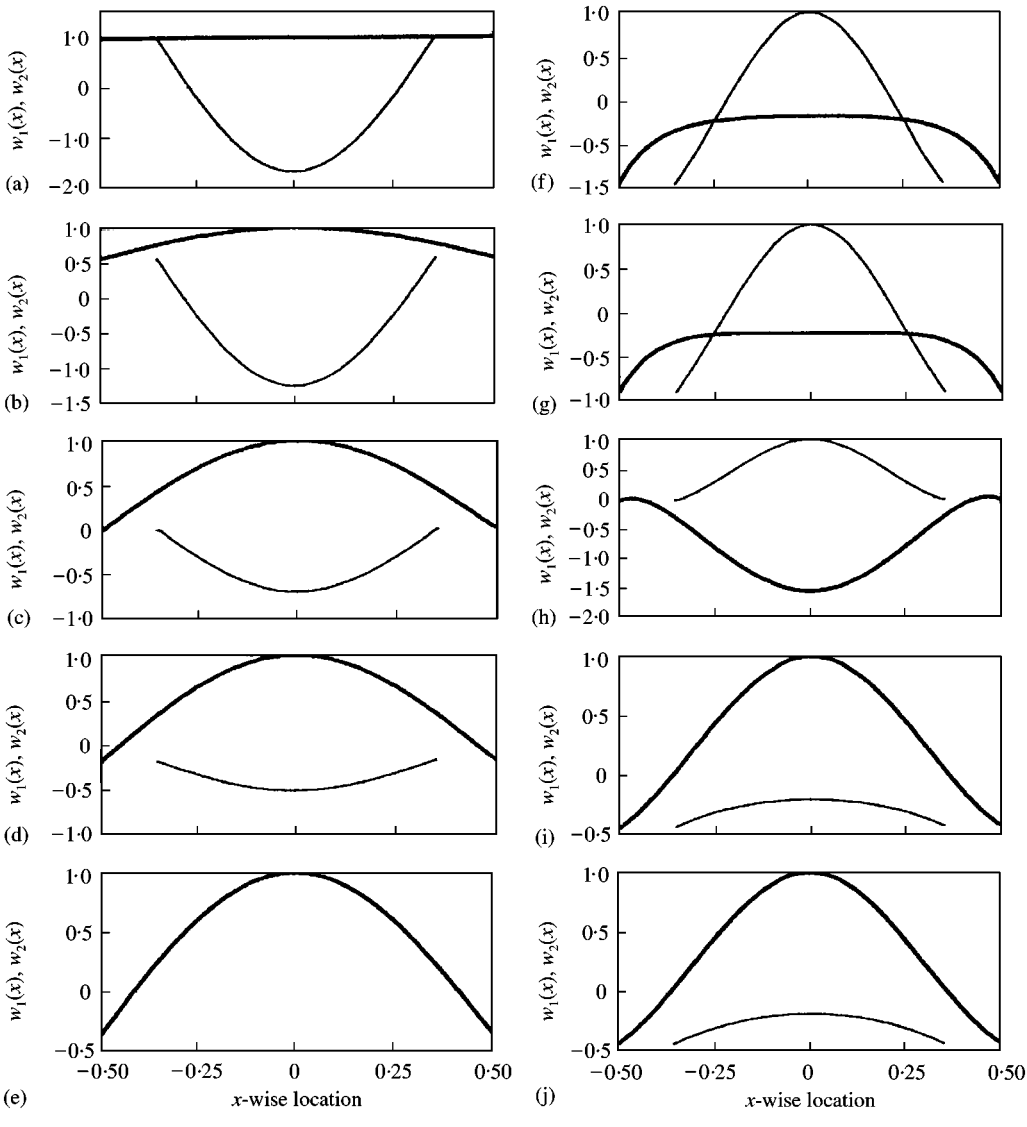

Figure 12. Flexural modes of square six-beam frames corresponding to points on the frequency curves of Figures 10 and 11, (a)–(e), Pin-jointed frame; (f)–(j), fixed-jointed frame. Long line, diagonal member; short line, side member. (a) $p = -56$; ND freq = 0·54; (b) $p = -46{\cdot}8$; ND freq = 14·56; (c) $p = -28{\cdot}24$; ND freq = 19·48; (d) $p = -16{\cdot}44$; ND freq = 18·0; (e) $p = 9{\cdot}84$; ND freq = 0·86; (f) $p = -116{\cdot}6$; ND freq = 0·141; (g) $p = -98{\cdot}77$; ND freq = 26·04; (h) $p = -67{\cdot}54$; ND freq = 40·00; (i) $p = -11{\cdot}01$; ND freq = 25·99; (j) $p = 26{\cdot}101$; ND freq = 0.12.

ends of the beam and over the central portion, the beam vibrates almost as a rigid body.

Notice also that the modes of the fixed-jointed frame at p-values of $-116{\cdot}6$ and $-98{\cdot}77$ are not significantly different, nor are those at p-values of $-11{\cdot}01$ and $26{\cdot}101$. Further mode calculations have shown that these modes change very little with changing p over most of the indicated range except in a small range close to $p = -67{\cdot}5$ where it is very rapid. Exactly the same phenomenon occurs with the fixed pair of beams but not with the pin-jointed frame or pinned beams.

5. CONCLUSIONS

Transcendental equations have been derived for the natural frequencies and modes of two simple redundant systems of straight uniform Euler–Bernoulli beams in which there are interacting internal self-balancing axial loads. The analysis has been restricted to symmetric mode vibrations normal to the plane of the symmetric systems. Frequencies and modes have been successfully computed for systems of pinned or fixed-jointed beams with equal or unequal flexural properties. The range of axial loads considered has extended well beyond the critical buckling loads of the beams, although it is recognized that this whole range may be unrealizable in practice.

When the axial load system first causes any one of the component beams to buckle, the fundamental frequency of the whole system vanishes. For systems of pinned beams, the critical compressive loads are given by the simple Euler buckling formula for each beam. Fixed beam systems are not fixed in an absolute sense so the critical loads cannot be given by simple formulae. They depend on the elastic restraining moments imposed by the adjacent beams.

Natural frequencies of the whole system may initially rise or fall as the compressive load in a member increases depending on the relative magnitudes of the buckling loads in the different members. If the fundamental frequency initially rises, the frequency of the next (higher) mode drops and *vice versa*. Such alternation is not necessarily followed by successively higher modes. A simple criterion which determines the rise or fall has been identified for the systems considered. The frequencies inevitably drop to zero as the axial loads continue to increase.

In the mode of vibration at a critical load condition (zero frequency), the buckled beam of a pinned system bends with a large amplitude while the unbuckled beam(s) move as rigid bodies. If the beams are fixed together, the buckled beam necessarily causes the unbuckled beam to bend but this is confined to the ends of the unbuckled beam. It moves almost as a rigid body over the middle part of the beam.

In each of the studied systems, the amplitudes of modal distortion at any axial load and frequency are greater in the compressed beam than in the stretched beam. The modes of the fixed-jointed beam pairs are exactly independent of the axial load when the pair have equal flexural stiffnesses and are still almost independent of axial load when the stiffnesses are not equal. An exception to this occurs when the axial load is in a narrow range close to the value which maximizes or minimizes the frequency, for then the mode changes very rapidly with changing load. These conclusions have all been drawn from studies on beam assemblies comprising members having flexural stiffness ratios between 0·5 and 2.

It has been established that quite small axial load changes in the structural members can significantly affect the natural frequencies of the system. In a multi-span truss structure, the axial loads in its members vary with the externally applied and thermal loads, with the member location and the amplitude of gross structural vibration. It may be concluded that high-frequency vibration transmission through, say, a space truss-type structure may be significantly affected by such parameter changes.

REFERENCES

1. LORD RAYLEIGH 1877 *Theory of Sound* (two volumes). New York: Dover Publications: second edition, 1945 re-issue.
2. S. P. TIMOSHENKO, D. H. YOUNG and W. WEAVER Jr 1974 *Vibration Problems in Engineering*, 453–455. New York: John Wiley; 4th edition.
3. C. L. AMBER-RAO 1967 *Journal of a Acoustical Society of America* **42**, 900–901. Effect of end conditions on the lateral frequencies of uniform straight columns.

4. A. E. GALEF 1968 *Journal of the Acoustical Society of America* **44**, 643. Bending frequencies of compressed beams.
5. D. J. GORMAN 1975 *Free Vibration Analysis of Beams and Shafts*, 359–381. New York: John Wiley.
6. R. D. BLEVINS 1979 *Formulas for Natural Frequencies and Mode Shapes*, 101–113. New York: Van Nostrand Reinhold.
7. F. W. WILLIAMS and J. R. BANERJEE 1985 *Journal of Sound and Vibration* **99**, 121–138. Flexural vibration of axially loaded beams with linear or parabolic taper.
8. A. BOKAIAN 1988 *Journal of Sound and Vibration* **126**, 49–65. Natural frequencies of beams under compressive axial loads.
9. N. G. STEPHEN 1989 *Journal of Sound and Vibration* **131**, 345–350. Beam vibration under compressive axial load—upper and lower bound approximation.
10. W. P. HOWSON and F. W. WILLIAMS 1973 *Journal of Sound and Vibration* **26**, 503–515. Natural frequencies of frames with axially loaded Timoshenko members.
11. A. BOKAIAN 1990 *Journal of Sound and Vibration* **126**, 481–498. Natural frequencies of beams under tensile axial loads.
12. S. WOINOWSKY-KRIEGER 1950 *Transactions of the American Society of Mechanical Engineers, Journal of Applied Mechanics* **72**, 35. The effect of an axial force on the vibrations of hinged bars.

APPENDIX A: EQUATIONS FOR THE BEAM DEFLECTION COEFFICIENTS

For the frame with pinned joints, the boundary conditions to be satisfied by the beam deflections are given by equations (25)–(27). By substituting into these the expressions for $w_1(x)$, $w_2(x)$, $w_3(x)$ from equations (9a–c) one obtains a 6×6 matrix equation of the form $[X][A, B, C]^{\mathrm{T}} = 0$ where $[A, B, C] = [A_1, A_2, B_1, B_2, C_1, C_2]$. The non-zero terms of the matrix $[X]$ are:

$$X_{1,1} = \cosh a_1/2, \quad X_{1,2} = \cosh a_2/2, \quad X_{1,3} = -\cosh \beta_1 l_{21}/2, \quad X_{1,4} = -\cosh \beta_2 l_{21}/2,$$

$$X_{2,1} = \cosh a_1/2, \quad X_{2,2} = \cosh a_2/2, \quad X_{2,5} = -\cosh \gamma_1 l_{31}/2, \quad X_{2,6} = -\cosh \gamma_2 l_{31}/2,$$

$$X_{3,1} = a_1^2 \cosh a_1/2, \quad X_{3,2} = a_2^2 \cosh a_2/2,$$

$$X_{4,3} = \beta_1^2 \cosh \beta_1 l_{21}/2, \quad X_{4,4} = \beta_2^2 \cosh \beta_2 l_{21}/2,$$

$$X_{5,5} = \gamma_1^2 \cosh \gamma_1 l_{31}/2, \quad X_{5,6} = \gamma_2^2 \cosh \gamma_2 l_{31}/2,$$

$$X_{6,1} = (a_1^3 + p a_1) \sinh a_1/2, \quad X_{6,2} = (a_2^3 + p a_2) \sinh a_2/2,$$

$$X_{6,3} = (e_{21}\beta_1^3 - p\beta_1 \cos\theta_2) \sinh \beta_1 l_{21}/2, \quad X_{6,4} = (e_{21}\beta_2^3 - p\beta_2 \cos\theta_2) \sinh \beta_2 l_{21}/2,$$

$$X_{6,5} = (e_{31}\gamma_1^3 - p\gamma_1 \cos\theta_3) \sinh \gamma_1 l_{31}/2, \quad X_{6,6} = (e_{31}\gamma_2^3 - p\gamma_2 \cos\theta_3) \sinh \gamma_2 l_{31}/2.$$

For the frame with fixed joints, the boundary conditions are expressed by equations (28)–(31) and these lead to the matrix equation $[Y]\lfloor A, B, C \rfloor^{\mathrm{T}} = 0$. The non-zero elements of $[Y]$ are:

$$Y_{1,1} = \cosh a_1/2, \quad Y_{1,2} = \cosh a_2/2, \quad Y_{1,3} = -\cosh \beta_1 l_{21}/2, \quad Y_{1,4} = -\cosh \beta_2 l_{21}/2,$$

$$Y_{2,1} = \cosh a_1/2, \quad Y_{2,2} = \cosh a_2/2, \quad Y_{2,5} = -\cosh \gamma_1 l_{31}/2, \quad Y_{2,6} = -\cosh \gamma_2 l_{31}/2,$$

$$Y_{3,1} = a_1 \sinh a_1/2, \quad Y_{3,2} = a_2 \sinh a_2/2,$$

$$Y_{3,3} = -\cos\theta_2\beta_1 \sinh\beta_1 l_{21}/2, \quad Y_{3,4} = -\cos\theta_2\beta_2 \sinh\beta_2 l_{21}/2,$$

$$Y_{3,5} = -\cos\theta_3\gamma_1 \sinh\gamma_1 l_{31}/2, \quad Y_{3,6} = -\cos\theta_3\gamma_2 \sinh\gamma_2 l_{31}/2,$$

$$Y_{4,1} = a_1^2 \cos\theta_2 \cosh a_1/2, \quad Y_{4,2} = a_2^2 \cos\theta_2 \cosh a_2/2,$$

$$Y_{4,3} = e_{21}\beta_1^2 \cosh\beta_1 l_{21}/2, \quad Y_{4,4} = e_{21}\beta_2^2 \cosh\beta_2 l_{21}/2,$$

$$Y_{5,1} = a_1^2 \cos\theta_3 \cosh a_1/2, \quad Y_{5,2} = a_1^2 \cos\theta_3 \cosh a_1/2,$$

$$Y_{5,5} = e_{31}\gamma_1^2 \cosh\gamma_1 l_{31}/2, \quad Y_{5,6} = e_{31}\gamma_2^2 \cosh\gamma_2 l_{31}/2,$$

$$Y_{6,1} = a_1^3 \sinh a_1/2, \quad Y_{6,2} = a_2^3 \sinh a_2/2,$$

$$Y_{6,3} = e_{21}\beta_1^3 \sinh\beta_1 l_{21}/2, \quad Y_{6,4} = e_{21}\beta_2^3 \sinh\beta_2 l_{21}/2,$$

$$Y_{6,5} = e_{31}\gamma_1^3 \sinh\gamma_1 l_{31}/2, \quad Y_{6,6} = e_{31}\gamma_2^3 \sinh\gamma_2 l_{31}/2.$$

When the frame has four identical side members $\theta_1 = \theta_2 = 45°$, $e_{21} = e_{31}$, $l_{21} = l_{31}$ and $B_1 = C_1$, $B_2 = C_2$ for the symmetric vibration modes. Together, these allow the matrix equation for the A's, B's and C's to be reduced to a 4×4 matrix equation $[X][A, B]^{\mathrm{T}} = 0$ where $\lfloor A, B \rfloor = \lfloor A_1, A_2, B_1, B_2 \rfloor$. The terms of $[X]$ are:

$$X_{1,1} = \cosh a_1/2, \quad X_{1,2} = \cosh a_2/2, \quad X_{1,3} = -\cosh\beta_1 l_{21}/2, \quad X_{1,4} = -\cosh\beta_2 l_{21}/2,$$

$$X_{2,1} = a_1 \sinh a_1/2, \quad X_{2,2} = a_2 \sinh a_2/2, \quad X_{2,3} = -2\beta_1 \cos 45° \sinh\beta_1 l_{21}/2,$$

$$X_{2,4} = -2\beta_2 \cos 45° \sinh\beta_2 l_{21}/2,$$

$$X_{3,1} = a_1^2 \cosh a_1/2, \quad X_{3,2} = a_2^2 \cosh a_2/2, \quad X_{3,3} = 2e_{21} \cos 45° \beta_1^2 \cosh\beta_1 l_{21}/2,$$

$$Y_{3,4} = 2e_{21} \cos 45° \beta_2^2 \cosh\beta_2 l_{21}/2,$$

$$Y_{4,1} = a_1^3 \sinh a_1/2, \quad Y_{4,2} = a_2^3 \sinh a_2/2, \quad Y_{4,3} = 2e_{21}\beta_1^3 \sinh\beta_1 l_{21}/2,$$

$$Y_{4,4} = 2e_{21}\beta_2^3 \sinh\beta_2 l_{21}/2.$$

APPENDIX B: NOMENCLATURE

A, B, C	coefficients of exponential or hyperbolic functions quantifying the beam displacements
e_{21}, e_{31}	the fractions EI_2/EI_1, EI_3/EI_1
EI_1, EI_2, EI_3	flexural rigidities of beams 1, 2, 3
m_1, m_2, m_3	mass per unit length of beams 1, 2, 3
p	non-dimensional axial load, Pl^2/EI_1 or Pl_1^2/EI_1
P	axial load in a beam
P_n	the nth critical buckling load of a beam
δP	the change of axial load in the beams due to differential shortening
t	time
$\delta u_{bending}$	the difference in shortening between two beams due to bending
w_1, w_2, w_3	transverse flexural displacement of beams 1, 2, 3
w_{max}	the maximum (central) deflection of a beam
x	spanwise co-ordinate along the length of a beam

$X(p, \Omega)$	non-dimensional function defined in equation (18b)
α, β, γ	non-dimensional wavenumbers of motion in beams 1, 2, 3
θ_2, θ_3	angles defining the frame geometry
κ	radius of gyration of a beam cross-section
μ_{21}, μ_{31}	the fractions $m_2/m_1, m_3/m_1$
ξ	non-dimensional spanwise co-ordinate, x/l or x/l_1
ω	circular frequency, rad/s
Ω	non-dimensional frequency, $m_1 l^4 \omega^2/EI_1$ or $m_1 l_1^4 \omega^2/EI_1$